ELSEVIER

Contents lists available at ScienceDirect

Journal of Molecular Liquids

journal homepage: www.elsevier.com/locate/mollig



Molecular simulations of adsorption of surfactant micelles on partially and fully covered iron surfaces



Abolfazl Faeli Qadikolae, Sumit Sharma*

Department of Chemical and Biomolecular Engineering, Ohio University, Athens, OH 45701, USA

ARTICLE INFO

Article history: Received 17 January 2023 Revised 23 February 2023 Accepted 18 March 2023 Available online 21 March 2023

Keywords: Surfactants Adsorption Metal-water interfaces Micelle Molecular simulation Free energy Molecular dynamics

ABSTRACT

Surfactant – metal interactions are important in applications like corrosion inhibition and synthesis of metallic nanoparticles, wherein surfactants are often added above their critical micelle concentration. Under these conditions, surfactant micelles exist in dynamic equilibrium with free surfactant molecules. Due to their faster diffusion compared to the micelles, free surfactant molecules rapidly adsorb onto metal-water interfaces. Therefore, adsorbing surfactant micelles invariably encounter metal-water interfaces with some adsorbed surfactants. We have studied, via atomistic simulations, adsorption behavior of micelles of a quaternary ammonium-based surfactant at iron-water interfaces that are partially or fully covered with adsorbed surfactant molecules. We find that on a partially covered surface, a micelle prefers to adsorb on a bare metal patch. On a fully covered surface, the micelle adsorbs on top of already adsorbed molecules and attains a hemispherical morphology. The adsorption free energy decreases as the coverage of iron-water interface with surfactants increases.

© 2023 Elsevier B.V. All rights reserved.

1. Introduction:

Adsorption of surfactants at metal-water interfaces is a facile way of altering the interfacial properties, and thus have found applications in corrosion inhibition [1-7], anisotropic growth of metallic nanoparticles [8-12], heterogeneous catalysis [13-16], and nanofabrication [17,18]. Surfactants, or surface-active agents, have a polar / hydrophilic head and a hydrophobic tail. At small concentrations, surfactants molecules exist in a dispersed phase in the aqueous environment. Above their critical micelle concentration (CMC), surfactants form micellar structures wherein the hydrophobic tails aggregate to minimize their exposure to water with the polar heads in contact with the aqueous phase. Many applications require surfactant solutions above their CMC [19.20]. For instance, in the synthesis of gold nanorods, concentration of CTAB molecules is close to 0.1 M which is much above their CMC [21,22]. Similarly, surfactants as corrosion inhibitors are effective in retarding corrosion at surface saturation concentration, which may be above the CMC [23,24]. Therefore, understanding surfactant adsorption at metal-water interfaces above the CMC is of significant interest. Free surfactant molecules, that is molecules that are not part of any micelle, adsorb on a metal surface strongly and with no free energy barrier, whereas ionic surfactant micelles

on partially/fully covered surfaces does not completely disinte-

grate. The micelle adsorbing on a fully covered metal surface

experience a free energy barrier to adsorption [25–29]. Furthermore, surfactant micelles have a much slower diffusion than the

free surfactant molecules [30]. The combined effect of these two

phenomena is that a surfactant micelle will invariably adsorb on

E-mail address: sharmas@ohio.edu (S. Sharma).

a metal surface that is already partially or fully covered with surfactants. Adsorption behavior of micelles on these surfaces is expected to be quite different than on bare metal surfaces. Previous works have also shown that when a surfactant micelle adsorbs on a bare metal-water interface, it disintegrates upon adsorption so that the constituent molecules spread of the surface [25]. In this work, we have studied, via molecular simulations, adsorption behavior of micelles of a quaternary ammonium-based surfactant with a 14 carbon long alkyl tail length, Quat-14 (Fig. 1), at metalwater interfaces that are either partially or fully covered with a layer of adsorbed Quat-14 molecules. We define a surface as fully covered when it does not have a large enough exposed metal region to adsorb a complete micelle. Our results show that on a partially covered metal surface, a surfactant micelle prefers to adsorb on the exposed metal surface. However, on a surface where the exposed metal surface area is not sufficient for a complete micelle to adsorb, adsorption of the micelle is dictated by hydrophobic interactions between the alkyl tail of the surfactants. Hence, in this scenario, the micelle adsorbs atop the first layer of adsorbed surfactant molecules. We find that a micelle adsorbing

^{*} Corresponding author.

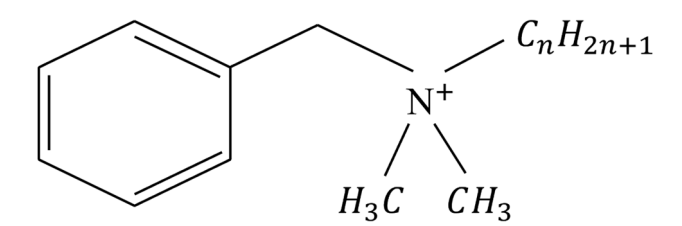


Fig. 1. Molecular structure of quaternary ammonium-based surfactant with 14 carbon long alkyl tail (n = 14), Quat-14.

attains a hemispherical morphology. In agreement with the previous studies, we observe that the micelles experience a free energy barrier to adsorption [25,31]. The adsorption free energy of the micelles is less favorable on the partially and the fully covered surfaces as compared to that on the bare metal surface.

2. Simulation system and methodology

Our simulation system comprises an iron surface submerged in water. The surface is prepared with different coverages of adsorbed surfactants using a procedure described later. Single Point Charge / Enhanced (SPC/E) water model is employed [32]. SPC/E is a widely used model that matches water's experimental liquid state density, diffusion constant, and radial distribution function. The iron surface is represented as a Body Centered Cubic (BCC) lattice with six layers since iron has BCC crystal structure at room temperature and pressure [33]. Interaction parameters of the iron surface with water and other species are taken from the Interface force field developed by Heinz group [34]. The iron surface is treated as charge neutral. Adsorption of a micelle of Quat-14 is studied by determining the free energy as a function of distance from the metal surface using umbrella sampling [35]. Partial charges on the Ouat-14 molecule are calculated by performing B3LYP level Density Functional Theory (DFT) with 6-31G(d.p) basis set in implicit water solvent using Gaussian 09 [36]. Interactions of Quat-14 are modeled by the General Amber Force Field (GAFF) [37]. Chloride ions are used as counter ions and their interaction parameters are taken from the Joung-Cheatham model [38]. Long range Coulombic interactions are calculated using Particle-Particle Particle Mesh Ewald summation. A spherical cutoff of 10 Å is chosen for Lennard Jones as well as the real space part of Coulombic interactions. We use PACKMOL to generate initial configurations of the simulation system [39].

Simulations are performed in the canonical ensemble (constant number of particles N, temperature T, and volume V) using the Nose-Hoover thermostat. The time-step of the simulations is chosen to be 2 fs (fs). Periodic boundary conditions (PBC) are applied in the x and y directions with the metal surface occupying the z = 0 plane. The opposite face of the simulation box has reflecting boundary condition to keep the system volume fixed. The simulation box size is taken as $L_x = L_y = 55$ Å and $L_z = 130$ Å. Above the water column, ~20 Å vacuum space is maintained to keep the system at saturation pressure at T = 300 K. A wall, which is reflective only to the surfactant molecules is placed 20 Å below the water column so as to prevent the surfactants from adsorbing at the vacuum-water interface. Iron atoms are kept frozen during the simulations as suggested in the Interface force field [34]. In addition to the above described simulation, we have performed isothermal-isobaric ensemble simulations to generate surfactant micelles in the aqueous phase. All simulations are performed using the Large-scale Atomic/Molecular Massively Parallel Simulator (LAMMPS) [40].

2.1. Adsorption free energy calculations

We have calculated the adsorption free energy of a Quat-14 micelle on iron surfaces that are partially or fully covered with adsorbed Quat-14 molecules using umbrella sampling [35]. For the umbrella sampling simulations, we choose center-of-mass distance of the micelle from the iron surface, ξ as the order parameter. The biasing potential is thus given by: $U(\xi,\xi_i)=\frac{1}{2}K(\xi-\xi_i)^2$, where K is the force constant, ξ is the set value of center-of-mass distance for the umbrella sampling window, and ξ_i is center-of-mass distance from the iron surface for a given configuration. The value of K is chosen to ensure that the adjacent umbrella sampling windows have sufficient overlap. The value of ξ is varied in different umbrella sampling windows so as to cover all distances from the interface to the bulk aqueous phase.

For obtaining a free energy profile, we generate over eighty overlapping umbrella sampling windows with $K=8.5~K_bT/\text{Å}^2$ for $\xi>15~\text{Å}$, $K=16.89~K_bT/\text{Å}^2$ for $10~\text{Å}<\xi<15~\text{Å}$, and for $\xi<10~\text{Å}$, we choose K between 40 and 250 $K_bT/\text{Å}^2$ to ensure good sampling of all values of ξ . We perform equilibration of each umbrella sampling window for 50 ns to 100 ns, and then perform three 10–20 ns production runs. The umbrella sampling bias is removed via the weighted histogram method (WHAM) to obtain the adsorption free energy profiles as a function of $\xi[41]$. We have performed umbrella sampling simulations using COLVARS package in LAMMPS [42]. We have also determined the adsorption free energy profile of a Quat-14 molecule in infinite dilution using umbrella sampling following a procedure similar to the one described above.

3. Results and discussion

3.1. Micelle adsorption on a partially covered iron surface

As a first step, we have studied adsorption of a Quat-14 molecule in infinite dilution at the iron-water interface. Similar to our previous results for the gold surface, we find that the Quat-14 molecule adsorbs strongly at the iron-water interface with an adsorption free energy of $40 \pm 1.73 \ k_B T$. The free energy profile shows no free energy barrier and the adsorbed molecule lies parallel to the surface (Fig. 2). Next, we investigate the adsorption behavior of surfactant micelles. To create a surface which is partially covered with surfactants, we randomly insert 20 Quat-14

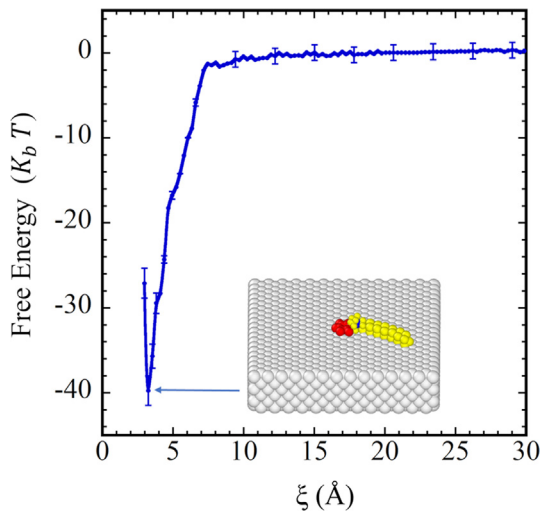


Fig. 2. Adsorption free energy of a Quat-14 surfactant in infinite dilution at the iron-water interface. Error bars are standard deviation in the free energy profile generated from three independent simulations.

molecules in the simulation box and equilibrate the system for 200 ns in the canonical ensemble (T = 300 K) to allow the molecules to adsorb on the surface and attain an equilibrium configuration. Only 8 surfactant molecules adsorb and the remaining form a micelle. The micelle remains in the bulk aqueous phase in the simulation. We perform the simulation for another 100 ns to ensure that no further adsorption occurs. This result is expected as we have shown in our previous work that ionic micelles have an appreciable free energy barrier to adsorption on metal surfaces [25,31].

The eight adsorbed surfactants aggregate in the adsorbed state and cover \sim 38% of the iron surface. We employ umbrella sampling methodology to study the adsorption free energy of the micelle on this partially covered surface. Since the umbrella sampling bias potential is applied only in the direction perpendicular to the plane of the surface, the micelle is free to diffuse parallel to the surface, that is along the x and y axes. Our simulations reveal that the micelle tends to adsorb onto the region with an exposed iron patch.

The free energy profile obtained from umbrella sampling is shown in the Fig. 3. There is a free energy barrier of $\sim 10 k_B T$ as the micelle approaches the surface. Our previous work has shown that this free energy barrier is associated with the perturbation of the spherically symmetric hydration shell of counterions that surround the micelle [25,29]. In our previous work, we have confirmed this assertion by showing that the free energy barrier disappears for a charge-neutral micelle wherein there are no counterions in the system [29]. Once this free energy barrier is overcome, two minimum in the free energy profile are observed. The local minimum at ~8 Å is associated with a solvent-seperated adsorbed configuration of the micelle. In this configuration, some polar groups do contact the metal surface but a layer of water prevents the alkyl tails from contacting the surface (Fig. 3). The global free energy minimum is observed at \sim 6 Å. In this configuration, the micelle is in contact with the surface with no solvent in-between. In this configuration, there is partial disintegration of the micelle. We speculate that the micelle disintegrates only partially because the entire iron

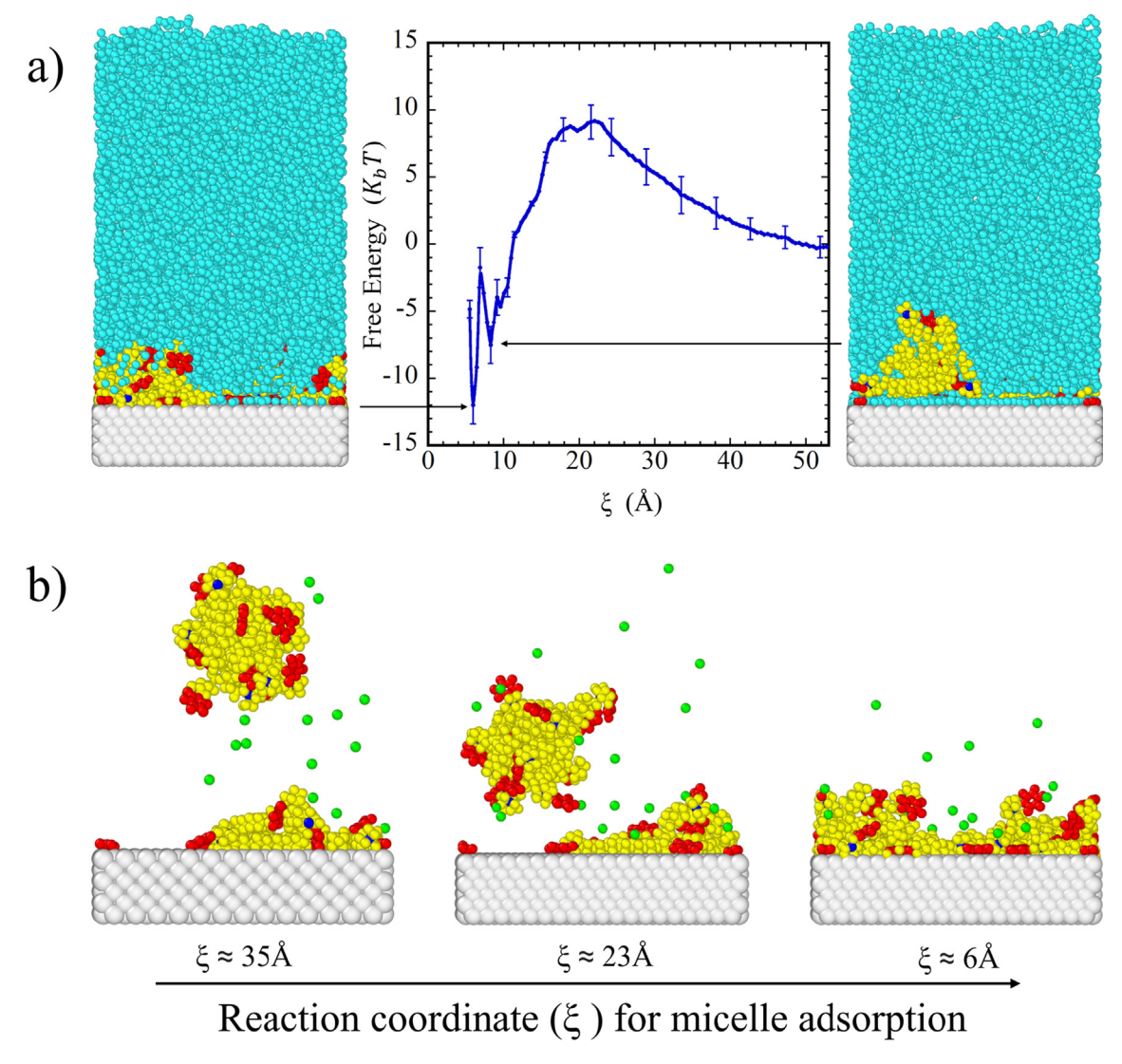


Fig. 3. a) Free energy profile of adsorption of a Quat-14 micelle on the iron surface that is partially covered by Quat-14 molecules as a function of distance of the micelle from the surface, ξ . Error bars are standard deviation in the free energy profile generated from three independent simulations. The snapshot on the left shows the configuration of the system at the global minimum of the free energy. The micelle is in contact with the surface. The snapshot on the right shows the configuration at the solvent-separated minimum. In the snapshots, the cyan colored beads represent water, the yellow beads represent the alkyl tail, and the red beads represent the polar head group. The grey beads represent the iron atoms. b) Snapshots from umbrella sampling windows associated with ξ = 35 Å, 23 Å and 6 Å. Water molecules have been removed for better visualization. Green beads represent the counterions. (For interpretation of the references to colour in this figure legend, the reader is referred to the web version of this article.)

surface is not available for it to spread and adsorb to form a monolayer. The overall adsorption free energy of the micelle is found to be $-13 \pm 1.5 \ k_B T$. After the adsorption of the micelle, the surface coverage increases from 38% to 78%. It is interesting to note that the solvent-separated local minimum in the free energy profile at \sim 8 Å observed here is absent in the free energy profiles associated with micelles adsorbing on gold surfaces. This is attributed to the stronger affinity of the iron surface for water as compared to the gold surface.

As the next step, we introduce another Quat-14 micelle in the simulation box to study its adsorption on the iron surface with the adsorbed surfactant coverage of 78%. On this surface, there is no bare patch of metal that is large enough to adsorb the entire micelle. Hence, we refer to this surface as fully covered with surfactants. For this step, we first generate a Quat-14 micelle by simulating Ouat-14 molecules in bulk water in an isothermal-isobaric simulation. Then we insert the micelle in our simulation system by removing appropriate number of water molecules so that the system size does not change. For this micelle, we employ the same umbrella sampling simulation procedure as described above to generate the adsorption free energy profile. Fig. 4 shows adsorption free energy profile of the second micelle. As before, there is a free energy barrier to adsorption of $\sim 10 k_B T$. Since the magnitude of the free energy barrier is similar to the one obtained for the first micelle, this implies that this barrier is not influenced by the nature of the surface. Location of the barrier associated with the second micelle shifts to a larger distance because the surface is now fully covered with surfactants. In contrast to the first micelle, we find that the second micelle prefers to adsorb on top of the already adsorbed surfactants. Therefore, when the surface is largely covered with surfactants, the hydrophobic interactions between the alkyl tails of the already adsorbed surfactants and the surfactants in the micelle dictate the adsorption process. As a result, the overall surface coverage does not change much after adsorption of the micelle (discussed later). It is also interesting to note that the free energy profile shows only a single minimum in the adsorbed state, that is there is no solvent separated free energy minimum.

Fig. 5 shows the surface coverage before and after the adsorption of micelles on the partially and fully covered surfaces. Inter-

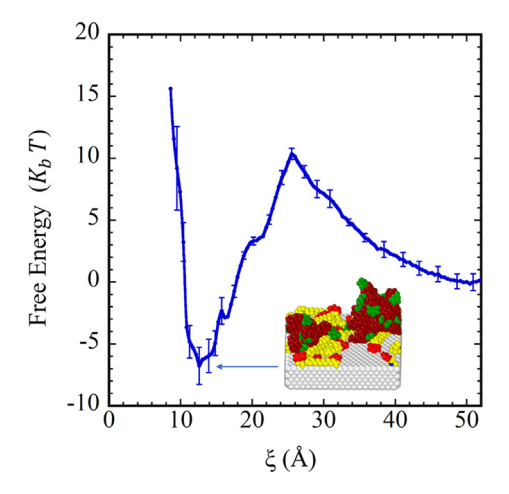


Fig. 4. Free energy profile of adsorption of a micelle on the iron surface that is covered with surfactant molecules. Error bars are standard deviation from three independent simulations. The inset shows a snapshot of the system at the free energy minimum. The brown and the green beads represent alkyl tail and the polar head group respectively of the surfactant molecules that form the micelle. The yellow and the red beads represent the alkyl tail and the polar head group respectively of the already adsorbed surfactants. The grey beads represent the iron atoms. (For interpretation of the references to colour in this figure legend, the reader is referred to the web version of this article.)

estingly, on the partially covered surface, the surface coverage jumps from 38% to 78% after the adsorption of the micelle, because the micelle adsorbs on the bare metal patch. On the other hand, on the fully covered surface, the surface coverage increases by <5% after adsorption of the micelle. This is so because the micelle adsorbs atop the already adsorbed surfactant molecules.

Fig. 6(a) shows the distributions of distance of the polar heads of surfactant molecules of the micelle adsorbed on the partially and the fully covered surfaces. The distributions are calculated when the micelle is at its free energy minimum in the adsorbed state. On the partially covered surface, there is a large peak in the distribution at \sim 3.5 Å, which shows that most surfactant molecules adsorb on the bare metal region of the surface. In contrast, on the fully covered surface, there is a much smaller peak at \sim 3.5 Å and a broad distribution at distances >10 Å, which implies that the micelle is adsorbing on top of the already adsorbed molecules and the micelle does not break upon adsorption. Fig. 6(b) shows the orientational distribution of the surfactants belonging to the micelle adsorbing on the partially and fully covered surfaces. The distributions are calculated when the micelles are at their free energy minimum in the adsorbed state. The angle θ is the angle that the alkyl tail of the surfactants makes with the surface normal. On the partially covered surface, there is a large peak at 90° implying that the surfactants prefer to lay parallel to the surface, similar to the configuration observed for a surfactant molecule adsorbing in infinite dilution. In the case of fully covered surfaces, the orientational distribution is broad for $\theta > 80^{\circ}$, which is indicative of a hemispherical configuration of the micelle. Interestingly, attainment of a hemispherical configuration by an adsorbing Quat micelle has previously been reported by us, wherein we employ an umbrella sampling based methodology to determine the most stable adsorbed morphology of the micelle [28].

Fig. 7 shows density profiles of water as function of distance from the surface that is associated with different locations of the micelle. When the micelle is far from the surface, water is strongly adsorbed in two distinct adsorbed layers. The peaks of the adsorbed layers of water decrease when the micelle is at the free energy minimum at \sim 8 Å on the partially covered surface, that is in the solvent-separately configuration. The peaks of the adsorbed layers of water further decrease when the micelle is at the global minimum at \sim 6 Å on the partially covered surface. The density profile of water does not drop significantly for the fully covered surface as compared to the partially covered case because

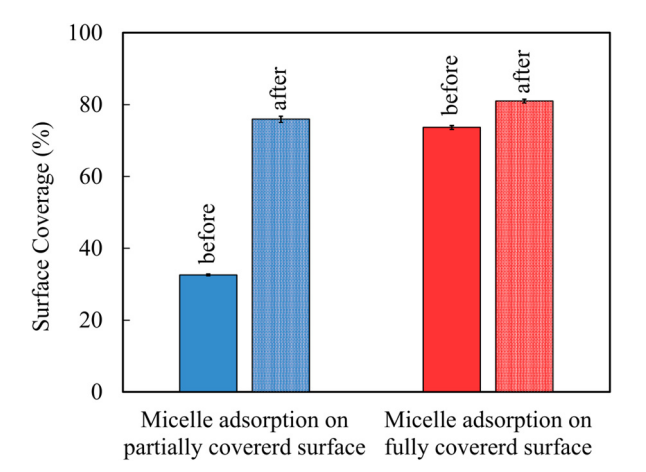


Fig. 5. Surface coverage before and after the adsorption of the micelle on a partially and a fully covered iron surface. On a partially covered surface, the micelle adsorbs on the bare metal patch, which results in a significant increase in the coverage. On the fully covered surface, the micelle adsorbs on top of the already adsorbed corrosion inhibitor molecules and the surface coverage does not increase much.

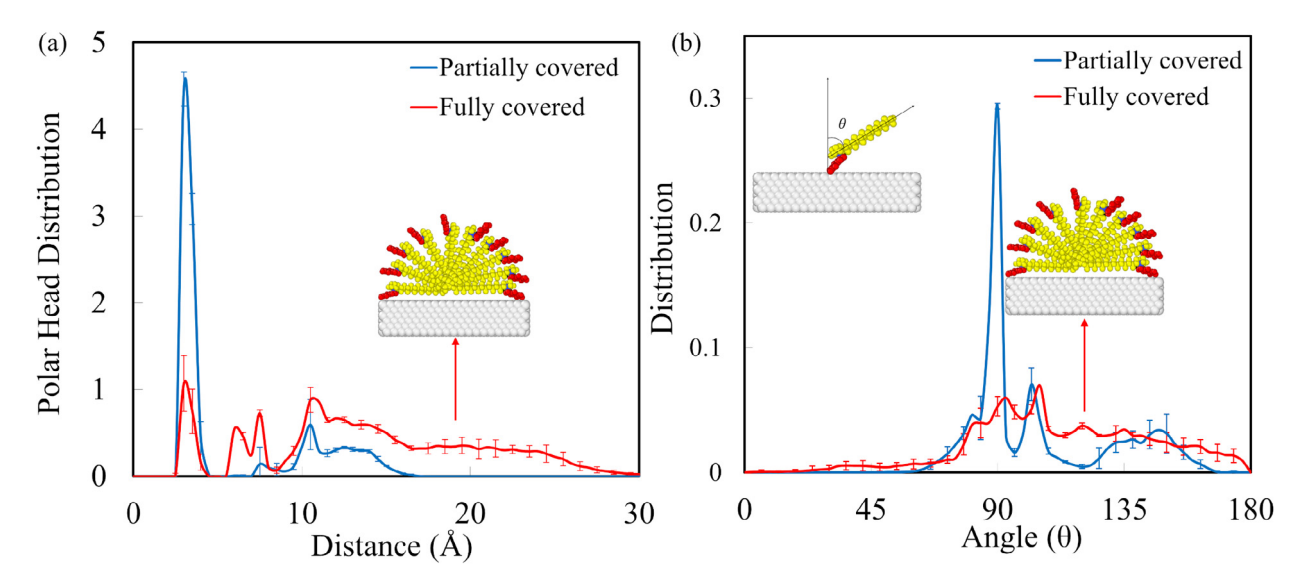


Fig. 6. (a) Distribution of distance of the polar heads, and (b) orientational distribution of surfactant molecules belonging to the micelle adsorbing on the partial and the fully covered surfaces. The distributions are calculated when the micelle is in the adsorbed state at the free energy minimum. θ is the angle that the alkyl tail makes with the surface normal [(b) inset]. The distribution in (b) is normalized by the number of adsorbed surfactant molecules and θ .

the surface coverage does not change much with the adsorption of the second micelle.

In the larger context of the phenomena of surfactant adsorption on solid interfaces, our work provides interesting insights. It is well established that hydrophobic interactions between the alkyl tails of surfactants not only impact the CMC in bulk aqueous phase, but also dictate the formation of well-packed adsorption mor-

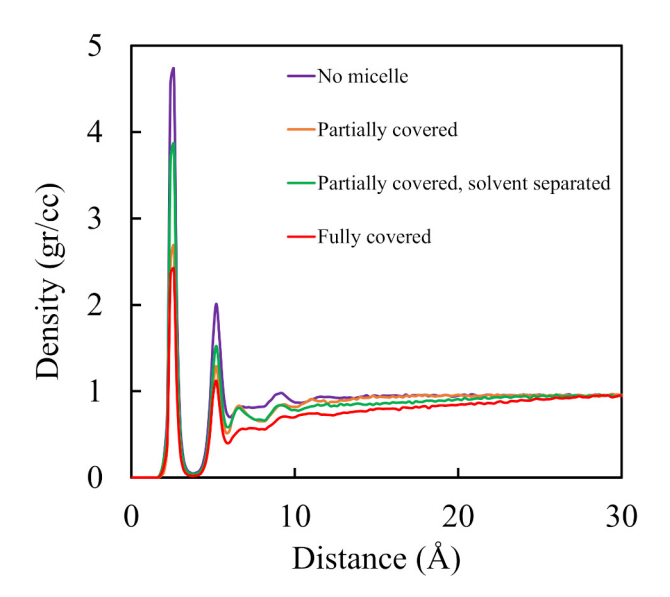


Fig. 7. Density profiles of water as function of distance from the surface. The 'No micelle' profile represents the case when the micelle is far from the surface and the surface is partially covered with surfactants. The 'Partially covered' profile represents the case when the micelle is adsorbed at its free energy minimum on the partially covered surface. The 'Partially covered, solvent separated' profile refers to the case when the micelle is in the solvent-separated configuration on the partially covered surface. The 'Fully covered' profile refers to the case when the micelle is adsorbed on the fully covered surface.

phologies [43–46]. This work highlights the role of hydrophobic interactions during the adsorption of micelles when the surfaces are partially or fully covered with surfactants. When the surface is only partially covered, the hydrophobic interactions cause the attainment of aggregated morphologies of adsorbed surfactants that leave behind bare metal patches. In contrast, on a fully covered surface, adsorption of the micelle is governed by the hydrophobic interactions between the alkyl tails of adsorbed surfactants and those in the micelle. While our work has studied the adsorption of pure surfactant micelles at metal-water interfaces, it can potentially be useful for envisioning the adsorption behavior of more complex systems, including the assemblies of surfactants with polymers and the self-assembled structures of block copolymers [47,48].

4. Conclusions

We have studied adsorption behavior of micelles of a quaternary ammonium-based surfactant (Quat-14) on iron-water interfaces that are partially or fully covered by Quat-14 molecules. We find that on a partially covered surface, the micelle prefers to adsorb on the bare metal patch. On a fully covered surface, the adsorption is driven by hydrophobic interactions between the alkyl tails of adsorbed inhibitor molecules and the molecules comprising the micelle. In this case, the micelle adsorbs on the surface in a hemispherical configuration. The adsorption free energy of the micelle decreases as the coverage of the surface with inhibitor molecules increases. In all cases, micelles experience a free energy barrier to adsorption.

CRediT authorship contribution statement

Abolfazl Faeli Qadikolae: Methodology, Software, Validation, Formal analysis, Investigation, Data curation, Writing – original draft, Visualization. **Sumit Sharma:** Conceptualization, Methodology, Resources, Writing – review & editing, Supervision, Project administration, Funding acquisition.

Data availability

Data will be made available on request.

Declaration of Competing Interest

The authors declare that they have no known competing financial interests or personal relationships that could have appeared to influence the work reported in this paper.

Acknowledgements

This work is supported by the NSF CAREER grant 2046095. Computational resources for this work were provided by Ohio Supercomputer Center (project number PAA0031), and NSF XSEDE grant DMR 190005.

References

- [1] M. Malik, M. Hashim, F. Nabi, S. Al-thabaiti, Z. Khan, Anti-corrosion ability of surfactants: a review, Int. J. Electrochem. Sci. 6 (2011).
- [2] M. Finšgar, J. Jackson, Application of corrosion inhibitors for steels in acidic media for the oil and gas industry: a review, Corros. Sci. 86 (2014) 17-41, https://doi.org/10.1016/j.corsci.2014.04.044.
- Y. Zhu, M.L. Free, R. Woollam, W. Durnie, A review of surfactants as corrosion inhibitors and associated modeling, Prog. Mater. Sci. 90 (2017) 159-223, https://doi.org/10.1016/j.pmatsci.2017.07.006.
- M. Aghaaminiha, R. Mehrani, M. Colahan, B. Brown, M. Singer, S. Nesic, S.M. Vargas, S. Sharma, Machine learning modeling of time-dependent corrosion rates of carbon steel in presence of corrosion inhibitors, Corros, Sci. 193 (2021). https://doi.org/10.1016/j.corsci.2021.109904.
- [5] M.H. Sliem, M. Afifi, A. Bahgat Radwan, E.M. Fayyad, M.F. Shibl, F.-E.-T. Heakal, A.M. Abdullah, AEO7 surfactant as an eco-friendly corrosion inhibitor for carbon steel in HCl solution, Sci. Rep. 9 (1) (2019) 2319, https://doi.org/ 10 1038/s41598-018-37254-7
- V.N. Ayukayeva, G.I. Boiko, N.P. Lyubchenko, R.G. Sarmurzina, R.F. Mukhamedova, U.S. Karabalin, S.A. Dergunov, Polyoxyethylene sorbitan trioleate surfactant as an effective corrosion inhibitor for carbon steel protection, Colloids Surf. Physicochem. Eng. Asp. 579 (2019), https://doi.org/ 10 1016/i colsurfa 2019 123636
- [7] M. Abdallah, M.A. Hegazy, M. Alfakeer, H. Ahmed, Adsorption and inhibition performance of the novel cationic Gemini surfactant as a safe corrosion inhibitor for carbon steel in hydrochloric acid, Green Chem. Lett. Rev. 11 (4) (2018) 457-468, https://doi.org/10.1080/17518253.2018.1526331
- [8] M. Luo, A. Ruditskiy, H.-C. Peng, J. Tao, L. Figueroa-Cosme, Z. He, Y. Xia, Pentatwinned copper nanorods: facile synthesis via seed-mediated growth and their tunable plasmonic properties, Adv. Funct. Mater. 26 (8) (2016) 1209-1216, nttps://doi.org/10.1002/adfm.201504217
- [9] C.J. Johnson, E. Dujardin, S.A. Davis, C.J. Murphy, S. Mann, Growth and form of gold nanorods prepared by seed-mediated. Surfactant-Directed Synthesis, J. Mater. Chem. 12 (6) (2002) 1765–1770, https://doi.org/10.1039/B200953F.
- [10] N. Jana, Z. Wang, T. Sau, T. Pal, Seed-mediated growth method to prepare cubic copper nanoparticles, Curr. Sci. 79 (2000).
- [11] Z. Qian, S.-J. Park, Silver seeds and aromatic surfactants facilitate the growth of anisotropic metal nanoparticles: gold triangular nanoprisms and ultrathin nanowires, Chem. Mater. 26 (21) (2014) 6172-6177, https://doi.org/10.1021
- [12] T. Song, F. Gao, S. Guo, Y. Zhang, S. Li, H. You, Y. Du, A review of the role and mechanism of surfactants in the morphology control of metal nanoparticles, Nanoscale 13 (7) (2021) 3895–3910, https://doi.org/10.1039/D0NR073390
- [13] H. Bönnemann, G. Braun, W. Brijoux, R. Brinkmann, A.S. Tilling, K. Seevogel, K. Siepen, Nanoscale colloidal metals and alloys stabilized by solvents and surfactants preparation and use as catalyst precursors, J. Organomet. Chem. 520 (1) (1996) 143–162, https://doi.org/10.1016/0022-328X(96)06273-0.
- [14] W. Zhan, Y. Shu, Y. Sheng, H. Zhu, Y. Guo, L. Wang, Y. Guo, J. Zhang, G. Lu, S. Dai, Surfactant-assisted stabilization of au colloids on solids for heterogeneous catalysis, Angew. Chem. Int. Ed. 56 (16) (2017) 4494-4498, https://doi.org/ 10.1002/anie.201701191
- [15] X. Feng, X. Lou, The effect of surfactants-bound magnetite (Fe3O4) on the photocatalytic properties of the heterogeneous magnetic zinc oxides nanoparticles, Sep. Purif. Technol. 147 (2015) 266–275, https://doi.org/ 10.1016/j.seppur.2015.04.036.
- [16] J.M. Thomas, W.J. Thomas, Principles and Practice of Heterogeneous Catalysis, John Wiley & Sons, 2014.
- [17] V.N. Urade, T.-C. Wei, M.P. Tate, J.D. Kowalski, H.W. Hillhouse, Nanofabrication of double-gyroid thin films, Chem. Mater. 19 (4) (2007) 768-777, https://doi. org/10.1021/cm062136n.

- [18] Y. Wang, A.E. DePrince, S.K. Gray, X.-M. Lin, M. Pelton, Solvent-mediated endto-end assembly of gold nanorods, J. Phys. Chem. Lett. 1 (18) (2010) 2692-2698, https://doi.org/10.1021/jz1010048.
- [19] G.B. Goh, D.M. Eike, B.P. Murch, C.L. Brooks, Accurate modeling of ionic surfactants at high concentration, J Phys Chem B 8 (2015).
- [20] E. Khamis, H.A. Al-Lohedan, A. Al-Mayouf, Z.A. Issa, Adsorption effect of cationic surfactants on corrosion inhibition of steel, Mater. Werkst. 28 (1) 1997) 46-50, https://doi.org/10.1002/mawe.19970280115.
- [21] B. Nikoobakht, M.A. El-Sayed, Preparation and growth mechanism of gold nanorods (NRs) using seed-mediated growth method, Chem. Mater. 15 (10) (2003) 1957-1962, https://doi.org/10.1021/cm0207321.
- [22] M.-Z. Wei, T.-S. Deng, Q. Zhang, Z. Cheng, S. Li, Seed-mediated synthesis of gold nanorods at low concentrations of CTAB, ACS Omega 6 (13) (2021) 9188-9195, https://doi.org/10.1021/acsomega.1c00510.
- [23] N. Moradighadi, S. Lewis, J.D. Olivo, D. Young, B. Brown, S. Nešić, Determining critical micelle concentration of organic corrosion inhibitors and its effectiveness in corrosion mitigation, Corrosion 77 (3) (2020) 266-275, https://doi.org/10.5006/3679.
- [24] M.L. Free, Understanding the effect of surfactant aggregation on corrosion inhibition of mild steel in acidic medium, Corros. Sci. 44 (12) (2002) 2865-2870, https://doi.org/10.1016/S0010-938X(02)00080-X.
- [25] H. Singh, S. Sharma, Disintegration of surfactant micelles at metal-water interfaces promotes their strong adsorption, J. Phys. Chem. B (2020), https:// doi.org/10.1021/acs.jpcb.9b10780.
- [26] A. Faeli Qadikolae, S. Sharma, Facet selectivity of cetyltrimethyl ammonium bromide surfactants on gold nanoparticles studied using molecular simulations, J. Phys. Chem. B 126 (48) (2022) 10249-10255, https://doi.org/ 10.1021/acs.ipcb.2c06236
- [27] S. Sharma, X. Ko, Y. Kurapati, H. Singh, S. Nešić, Adsorption behavior of organic corrosion inhibitors on metal surfaces-some new insights from molecular simulations, Corrosion 75 (1) (2018) 90-105, https://doi.org/10.5006/2976.
- H. Singh, S. Sharma, Determination of equilibrium adsorbed morphologies of surfactants at metal-water interfaces using a modified umbrella samplingbased methodology, J. Chem. Theory Comput. 18 (4) (2022) 2513-2520, https://doi.org/10.1021/acs.jctc.2c00078
- [29] H. Singh, S. Sharma, Free energy profiles of adsorption of surfactant micelles at metal-water interfaces, Mol. Simul. 47 (5) (2021) 420-427, https://doi.org/
- [30] D.W. Armstrong, T.J. Ward, micellar effects on molecular diffusion: theoretical and chromatographic considerations, Anal. Chem. 58 (3) (1986) 579-582, https://doi.org/10.1021/ac00294a019.
- [31] Y. Kurapati, S. Sharma, Adsorption free energies of imidazolinium-type surfactants in infinite dilution and in micellar state on gold surface, J. Phys. Chem. B 122 (22) (2018) 5933–5939, https://doi.org/10.1021/acs.jpcb.8b02358.
- [32] H.J.C. Berendsen, J.R. Grigera, T.P. Straatsma, The missing term in effective pair potentials, J. Phys. Chem. 91 (24) (1987) 6269–6271, https://doi.org/10.1021/ i100308a038.
- [33] R.E. Smallman, A.H.W. Ngan, Physical Metallurgy and Advanced Materials, Elsevier, 2011.
- [34] K. Kanhaiya, S. Kim, W. Im, H. Heinz, Accurate simulation of surfaces and interfaces of ten FCC metals and steel using Lennard-Jones potentials, Npj Comput. Mater. 7 (1) (2021) 1-15, https://doi.org/10.1038/s41524-020
- [35] G.M. Torrie, J.P. Valleau, Nonphysical sampling distributions in monte carlo free-energy estimation: umbrella sampling, J. Comput. Phys. 23 (2) (1977) 187–199, https://doi.org/10.1016/0021-9991(77)90121-8.
 [36] M. Caricato, Æ. Frisch, J. Hiscocks, M.J. Frisch, Gaussian 09 IOps Reference
- Second Edition Edited By.
- [37] J. Wang, R.M. Wolf, J.W. Caldwell, P.A. Kollman, D.A. Case, Development and testing of a general amber force field, J. Comput. Chem. 25 (9) (2004) 1157-1174, https://doi.org/10.1002/jcc.20035.
- [38] I.S. Joung, T.E. Cheatham, Determination of alkali and halide monovalent ion parameters for use in explicitly solvated biomolecular simulations, J. Phys. Chem. B 112 (30) (2008) 9020–9041, https://doi.org/10.1021/jp8001614.
- PACKMOL: A package for building initial configurations for molecular dynamics simulations Martínez 2009. J. Comput. Chem. Wiley Online Library. https://onlinelibrary.wiley.com/doi/full/10.1002/jcc.21224 (accessed 2022-08-02).
- S. Plimpton, Fast parallel algorithms for short-range molecular dynamics, J. Comput. Phys. 117 (1) (1995) 1-19, https://doi.org/10.1006/jcph.1995.1039.
- [41] M. Souaille, B. Roux, Extension to the weighted histogram analysis method: combining umbrella sampling with free energy calculations, Comput. Phys. Commun. 135 (1) (2001) 40-57, https://doi.org/10.1016/S0010-4655(00)
- [42] G. Fiorin, M.L. Klein, J. Hénin, Using collective variables to drive molecular dynamics simulations, Mol. Phys. 111 (22-23) (2013) 3345-3362, https://doi. org/10.1080/00268976.2013.813594.
- [43] X. Ko, S. Sharma, A quantitatively accurate theory to predict adsorbed configurations of asymmetric surfactant molecules on polar surfaces, J. Phys. Chem. B 124(26)(2020) 5517–5524, https://doi.org/10.1021/acs.jpcb.0c02681.
- S. Sharma, H. Singh, X. Ko, A quantitatively accurate theory to predict adsorbed configurations of linear surfactants on polar surfaces, J. Phys. Chem. B 123 (34) (2019) 7464-7470, https://doi.org/10.1021/acs.jpcb.9b05861.

- [45] M.R. Khan, H. Singh, S. Sharma, K.L. Asetre Cimatu, Direct observation of adsorption morphologies of cationic surfactants at the gold metal-liquid interface, J. Phys. Chem. Lett. 11 (22) (2020) 9901–9906, https://doi.org/ 10.1021/acs.jpclett.0c02517.
- [46] X. Ko, S. Sharma, Adsorption and self-assembly of surfactants on metal-water interfaces, J. Phys. Chem. B 121 (45) (2017) 10364–10370, https://doi.org/10.1021/acs.jpcb.7b09297.
- [47] X. Wang, K. Hong, D. Baskaran, M. Goswami, B. Sumpter, J. Mays, Asymmetrical self-assembly from fluorinated and sulfonated block copolymers in aqueous media, Soft Matter 7 (18) (2011) 7960–7964, https://doi.org/10.1039/ C1SM06040F.
- [48] J.M. Borreguero, P.A. Pincus, B.G. Sumpter, M. Goswami, Unraveling the agglomeration mechanism in charged block copolymer and surfactant complexes, Macromolecules 50 (3) (2017) 1193–1205, https://doi.org/ 10.1021/acs.macromol.6b02319.